

Stable and erasable patterning of vanadium pentoxide thin films by atomic force microscope nanolithography

Shiho Iwanaga and R. B. Darling

Department of Electrical Engineering, University of Washington, Seattle, Washington 98195

D. H. Cobden

Department of Physics, University of Washington, Seattle, Washington 98195

(Received 27 September 2004; accepted 14 February 2005; published online 25 March 2005)

Long lasting colored pattern formation on sol-gel deposited vanadium pentoxide (V_2O_5) thin films is demonstrated by atomic force microscope (AFM) nanolithography. The films can be locally colorized by application of a positive dc bias voltage on the conductive AFM tip. The patterns can be erased, or "bleached," by application of a negative bias voltage. The changes in optical reflectivity, topography, and conductivity measurements made on as-deposited, colored, and bleached areas were consistent with a model in which the incorporation of hydrogen ions into V_2O_5 thin films is responsible for the coloration process. © 2005 American Institute of Physics. [DOI: 10.1063/1.1896100]

Atomic force microscope (AFM) nanolithography is a promising method for creating nano-scale patterns for applications such as nanometer-scale device fabrication or very high density memory storage systems.^{1,2} It is known that application of an appropriate bias voltage to a conductive AFM tip can induce electrochemical reactions directly on the material surfaces.³ In oxidation pattern formation on passivated semiconductor or metal surfaces,⁴ for example, the tip bias creates a strong electric field ($>10^7$ V/cm), which enhances the diffusion of oxyanions (O^- , OH^-), anodically oxidizing the substrate beneath the tip.⁵ In this method, however, the created patterns on the substrate are chemically unstable, limiting their utility. The bare substrate forms a native oxide: thus, the fabricated oxide patterns fade away over time.^{6,7} Developing a new nanolithography system that overcomes such problems would be of great interest, especially for applications that requires long lasting patterns. In the present study, AFM nanolithography has been applied to a transition metal oxide, specifically V_2O_5 , introducing a method to generate stable patterns.

V_2O_5 is thermodynamically stable at atmospheric oxygen partial pressures up to its melting point.⁸ V_2O_5 is known as an electrochromic material, owing to its layered structure that makes it a good ion conductor, as well as a high capacity ion storage medium.⁹ Under appropriate voltage bias, V_2O_5 changes color reversibly in multiple steps, which is caused by a number of abrupt changes in the absorption band locations, as a result of forming stable phases with intercalated positive ions (e.g., Li^+).¹⁰ With this unique property, V_2O_5 thin films can be employed for various applications such as smart windows and information displays.^{11,12} It has been shown that the optical properties of V_2O_5 thin films can be altered by several other methods including thermal treatment,¹³ ion or electron bombardment,¹⁴ and laser irradiation.¹⁵ Here, we have successfully applied an AFM nanolithography method to V_2O_5 thin films and generated local coloration, which can be erased. Conductivity, topography, and optical reflectivity measurements were carried out on as-deposited, colored, and bleached areas of the V_2O_5 thin films.

The V_2O_5 thin films were produced by a sol-gel method, described by Ozer.¹⁶ Using vanadium oxide isopropoxide [$VO(i-OC_2H_5)_3$] (Alfa Aesar) as a precursor, the bright orange sol was first prepared. The substrate was a silicon wafer with a 100 nm chromium layer predeposited by e-beam evaporation, as a bottom electrode. The substrates were cleaned by acetone in a sonicator, followed by rinsing in deionized water and isopropyl alcohol. The substrate was dipped into the sols using a dip coater, with a dipping rate of ~ 5 cm/s. Four coatings were made in succession to increase the thickness. After each dipping, the specimen was annealed in a furnace at 250 °C for 10 min to avoid dissolution of the previous coatings. Final curing was performed at 500 °C for 10 min. X-ray diffraction analysis indicated that the film had a crystalline structure, with a preferred orientation of the (001) planes lying parallel to the substrate surface. The thickness was approximately 85 nm, as measured by the AFM from a sharp step created by nitric acid etching. Interference effects largely influence the apparent color of the film. The film prepared for this study had a transparent light yellow color, and was uniform over the sample.

In ambient, a commercial AFM (Nanoscope 3100, Digital Instruments) was operated in contact mode to create patterns on the V_2O_5 film. A dc bias was applied to the tip that serves as a top electrode, and the current flowing from the tip to the film was monitored using a current amplifier. A platinum coated cantilever with nominal tip radius of 30 nm, spring constant 1.0 N/m, and resonant frequency 25 kHz was used. As the tip scanned over the surface in mechanical contact with the film surface, the normal force was kept around 50 nN, the minimum force required to maintain a good electrical contact.

Figure 1(a) is an optical microscope image of the colored (location 1) and subsequently bleached (location 2) regions, and Fig. 1(b) is the corresponding topography. This pattern was created in two steps as in Fig. 1(c). First, the tip was scanned over the vertical rectangular area ($15 \times 5 \mu m^2$) while applying bias voltage of +6 V with respect to the chromium-coated substrate. The coloration change from light yellow to blue-green could be observed instantaneously at the region under the tip scanning at 5 $\mu m/s$. Sec-

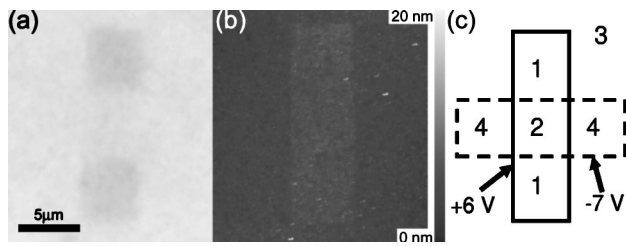


FIG. 1. (a) Optical microscope photograph of the colored and bleached area, and (b) the topography. Scheme of the locations where voltages were applied is shown in (c). First, the area surrounded by the solid line was raster scanned with +6 V bias, followed by the -7 V bias scan in the area surrounded by the broken line. Numbers 1–4 indicate location number.

ond, the tip scanned over the horizontal rectangular area ($5 \times 15 \mu\text{m}^2$) with a tip bias of -7 V. The blue-green color at location 2 has been erased, or almost fully recovered to its original yellow color as at location 3, and we refer to this therefore as “bleaching.” Note that negative bias voltage applied to the as-deposited areas does not cause any color change (location 4). These results show that the blue-green coloration of the film is induced only by a positive bias voltage. Negative bias voltages induce color change only at the blue-green colored regions, which makes the procedure appear to “bleach” the blue-green color. These colors maintain clear contrast even after the voltage application is terminated. The patterns last for months in air.

The topographic image in Fig. 1(b) was taken in tapping mode AFM, by connecting the same tip to the ground. This image reveals that the coloration procedure has caused an increase in height of about 2–4 nm (2.5%–4.5%). The bleaching procedure does not appear to reverse the thickness. Note that the increase in the topography was not due to physical damage such as scratching by the tip: the increase in height was not observed for the low bias voltages that do not induce coloration.

Optical reflectivity measurements were made in the as-deposited, colored, and bleached regions in the wavelength range 430–650 nm in Fig. 2. Larger areas for colored and bleached regions were created ($60 \times 60 \mu\text{m}^2$) for simplifying the measurements. The reflectivity spectrum measured on the as-deposited region, or “as-deposited” reflectivity, shows a feature in the range of 460–650 nm. Reflectivity calculations,¹⁷ using the reported values of $n(\lambda)$ and $k(\lambda)$,¹⁶ and the measured film thickness, confirm that this is a part of the primary constructive interference fringe. The spectrum shifts to shorter wavelength in the colored region. This shift

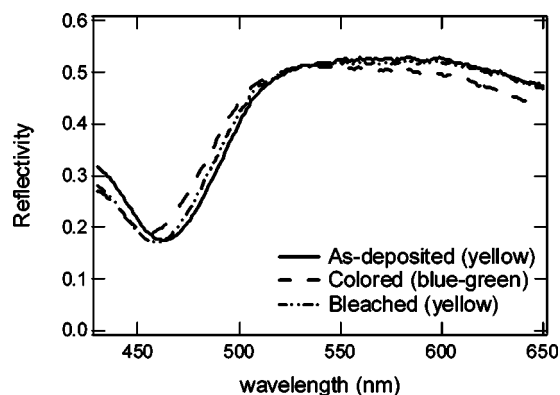


FIG. 2. Reflectivity of as-deposited, colored, and bleached regions.

Downloaded 01 May 2005 to 128.95.104.58. Redistribution subject to AIP license or copyright, see <http://apl.aip.org/apl/copyright.jsp>

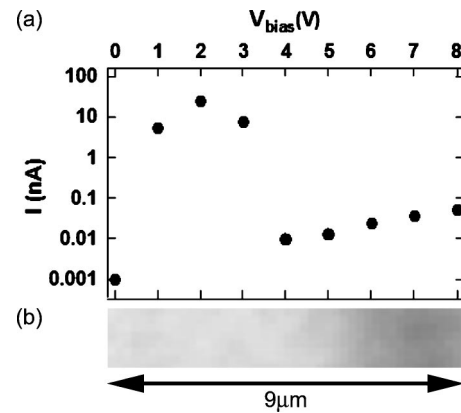


FIG. 3. (a) Average current vs tip bias voltage of coloration and (b) optical microscope photograph.

resulted in the reduction of reflectivity in the yellow to red range (530 nm–650 nm) by about 4%, and an increase in the blue to green range (460–530 nm) by about 6%. The spectrum in the bleached region has been nearly restored to that in the as-deposited region. These results suggest that the spectral shift of the reflectivity in the interference range causes the apparent color reversibility.

In the highly absorbing region (430–460 nm) where the reflectivity is low, the “colored” reflectivity spectrum also shows a shift to shorter wavelengths. Note that, in spite of the drastic apparent color change after the bleaching process, the “bleached” reflectivity did not recover to the “as-deposited” reflectivity. This confirms that the apparent color is determined mostly by the reflectivity in the interference region, instead of this highly absorbing region.

To obtain additional clues as to the coloration mechanism, an electrical conductivity measurement was carried out during the coloration process. The current through the tip provides information about local electrical properties, which are difficult to obtain using traditional deposited thin film metal contact methods. The average current flowing into the film following the application of incremental bias voltages (0, +1, +2, ..., +8 V) is shown in Fig. 3(a), and the corresponding optical microscope image of the film surface in Fig. 3(b). For biases up to 2 V, a current flows whose magnitude is consistent with the expected spreading resistance¹⁸ of V_2O_5 , whose bulk resistivity is $0.27 \Omega \cdot \text{m}$.¹⁹ Further increase of the bias causes an abrupt decrease in the current. At 4 V, the film has increased in resistivity by several orders of magnitude ($>10^2$). Figure 3(b) reveals that coloration occurs only above a threshold of about +6 V. This result indicates that the coloration is accompanied by a significant decrease in the conductivity of the film. The conductivity remains low after the bleaching process. For the case shown in Fig. 1, the current through the film (location 2) during the application of -7 V was less than -1 pA. This suggests that the resistance remains very high, in spite of the recovery of the color on bleaching.

The AFM coloration of the film is not a result of reflectivity changes caused by the increase in thickness. As the increase in film thickness is only a few nm, the calculations¹⁷ indicate that the increase in film thickness has a minimal effect, on the reflectivity, of less than 1%. Additionally, we see no change in the surface roughness which might influence the scattering. We argue that the AFM coloration of the V_2O_5 film results from the injection of H^+ ions and the con-

sequent changes in the electronic structure of the film. It has been reported that the new V_2O_5 phase incorporating the injected H^+ ions in crystalline V_2O_5 results in the expansion of the volume by a factor of 1.0%–4.5%.²⁰ Also, a decrease in the conductivity by a factor of 10^1 – 10^2 occurs due to the reduction of the carrier mobility caused by higher polaron density.²¹ This can explain both the change in height [Fig. 1(b)] and decrease in conductivity [Fig. 3(a)] of the colored region. Further, another study shows that the disturbance of the V_2O_5 structure by intercalated hydrogen atoms causes a blueshift of the absorption band,²² which is located in the spectrum range up to ~ 530 nm. In Fig. 2, the absorption band shift is inferred from the reflectivity spectrum shift in the absorbing band region (~ 530 nm). The reflectivity calculation used previously shows that the blue shift of the “colored” reflectivity spectrum in this range is caused by the blueshift of n and k components of the refractive index. This suggests a blueshift of the absorption band, since the absorption coefficient is proportional to k ($\alpha = 4\pi k/\lambda$).

Presumably, H^+ ions present in the water meniscus around the tip are injected into the V_2O_5 film, which is enhanced by the high electric field at the tip- V_2O_5 film interface. Indeed, the injected charge density during the coloration process is similar to the density of unit cells in the film, consistent with injection of few protons per unit cell. This suggests that the coloration process is of an electrochemical nature. On the other hand, the “bleaching” process is not merely a reversal of the “coloration” process (i.e., extraction of hydrogen), since an opposite current is not required for the bleaching process ($I < -1$ pA). This is shown by the conductance, topography, and the reflectivity in the highly absorbing region each does not recover to the “as-deposited” conditions. Some other process, such as field-induced polarization, may be occurring.

In summary, AFM lithography was demonstrated to induce stable, erasable color patterns on V_2O_5 thin films, which last for months under ambient air conditions. It was shown that the coloration of the V_2O_5 thin film, by application of a positive tip voltage, causes various physical changes including a volume increase, a drastic decrease in the conductivity, and a shift of the reflectivity spectrum. We suggest that the AFM coloration process of the V_2O_5 film involves the intercalation of H^+ ions. The bleaching process,

produced by a negative tip bias voltage, showed no changes in the volume, conductivity or reflectivity spectrum in the high absorption region. However, a shift in the reflectivity spectrum was induced at the primary interference fringe, causing the apparent film color to revert to close to its original color.

The authors would like to thank Professor F. S. Ohuchi and Dr. Taisuke Ohta for fruitful discussions.

¹Hyongsok T. Soh, Kathryn Wilder Guarini, and Calvin F. Quate, *Scanning Probe Lithography* (Kluwer Academic, Boston, 2001).

²R. Imura, H. Koyanagi, M. Miyamoto, A. Kikukawa, T. Shintani, and S. Hosaka, *Microelectron. Eng.* **27**, 105 (1995).

³Phaedon Avouris, Tobias Hertel, and Richard Martel, *Appl. Phys. Lett.* **71**, 285 (1997).

⁴Hirofumi Sugimura, Tatsuya Uchida, Noboru Kitamura, and Hiroshi Masuhara, *J. Phys. Chem.* **98**, 4352 (1994).

⁵E. S. Snow and P. M. Campbell, *Appl. Phys. Lett.* **64**, 1932 (1994).

⁶Sorab K. Ghandhi, *VLSI Fabrication Principles* (Wiley-Interscience, New York, 1994).

⁷D. Gräf, M. Grundner, and R. Schulz, *J. Vac. Sci. Technol. A* **7**, 808 (1989).

⁸D. Morris, R. Dixon, F. H. Jones, Y. Dou, R. G. Egdell, S. W. Downes, and G. Beamson, *Phys. Rev. B* **55**, 16083 (1997).

⁹A. E. Semenov, I. N. Borodina, and S. H. Garofalini, *J. Electrochem. Soc.* **148** A1239 (2001).

¹⁰M. Benmoussa, A. Outzourhit, A. Bennouna, and E. L. Ameziane, *Thin Solid Films* **405**, 11 (2002).

¹¹Yoshitaka Fujita, Katsuhiko Miyazaki, and Chie Tatsuyama, *Jpn. J. Appl. Phys., Part 1* **24**, 1082 (1995).

¹²M. Benmoussa, E. Ibnouelghazi, A. Bennouna, and E. L. Ameziane, *Thin Solid Films* **265**, 22 (1995).

¹³A. I. Gavriluk, N. M. Reinov, and F. A. Chudnovskii, *Sov. Tech. Phys. Lett.* **5**, 514 (1979).

¹⁴H. M. Naguib and R. Kelly, *J. Phys. Chem. Solids* **33**, 398 (1972).

¹⁵E. E. Khawaja, M. A. Khan, F. F. Al-Adel, and Z. Hussain, *J. Appl. Phys.* **68**, 1205 (1990).

¹⁶Nilgün Özer, *Thin Solid Films* **87**, 305 (1997).

¹⁷H. A. Macleod, *Thin-Film Optical Filters* (Institute of Physics, Philadelphia, 2001).

¹⁸P. De Wolf, J. Snauwaert, L. Hellemans, T. Clarysse, W. Vandervorst, M. D’Olieslaeger, and D. Quaechehaegens, *J. Vac. Sci. Technol. A* **13**, 1699 (1995).

¹⁹G. V. Samsonov, *The Oxide Handbook* (IFI/Plenum, New York, 1992).

²⁰A. Yoshikawa, K. Yagisawa, and M. Shimoda, *J. Mater. Sci.* **29**, 1319 (1994).

²¹M. Shimoda, A. Yoshikawa, and K. Yagisawa, *J. Mater. Sci.* **29**, 478 (1994).

²²Alexander Gavriluk, *Proc. SPIE* **2968**, 195 (1997).